This document was prepared in conjunction with work accomplished under Contract No. DE-AC09-96SR18500 with the U.S. Department of Energy.

This work was prepared under an agreement with and funded by the U.S. Government. Neither the U. S. Government or its employees, nor any of its contractors, subcontractors or their employees, makes any express or implied: 1. warranty or assumes any legal liability for the accuracy, completeness, or for the use or results of such use of any information, product, or process disclosed; or 2. representation that such use or results of such use would not infringe privately owned rights; or 3. endorsement or recommendation of any specifically identified commercial product, process, or service. Any views and opinions of authors expressed in this work do not necessarily state or reflect those of the United States Government, or its contractors, or subcontractors.

Proceedings of PVP2008
2008 ASME Pressure Vessels and Piping Division Conference
July 27-31, 2007, Chicago, Illinois, USA

PVP2008-61130

Fluid Transients in a Pipeline With One Open End

Robert A. Leishear
Savannah River National Laboratory
Aiken, South Carolina, 29803
803-725-2832, Robert.Leishear@SRS.gov

ABSTRACT

Water hammer during multi-phase flow is rather complex, but in some cases an upper limit to the pressure surge magnitude during water hammer can be estimated. In the case considered here, a two mile long pipeline with a single high point was permitted to partially drain. Due to gravitational effects, air bubbles up through the pipe line to its highest point, but the time required for air to reach the top of the pipe is rather long. Consequently, some transients caused by valve operations are affected by air entrapment and some are not. The intent of this research was to investigate the complex interactions between air, water vapor, and liquid during water hammer in a long pipe with one end of the pipe open to atmospheric conditions. To understand the system dynamics, experimental data was obtained from a long pipeline with an open end and also from a short, transparent tube. Transient calculations were performed for valve closures and pump operations as applicable. The limitations of available calculation techniques were considered in detail.

KEYWORDS

Water hammer, two phase flow, air entrainment.

SYMBOLS

a	shock velocity, feet/second
g	gravitational constant, feet/ sec^2
k	bulk modulus, psi
K	friction coefficient
D	diameter, inches
E	modulus of elasticity, psi
ID	inside diameter, inches
NPS	nominal pipe size
OD	outside diameter, finches
psi	pounds per square inch
P	pressure, psi
V	velocity, feet / second
t	pipe wall thickness, inches
Z	elevation, feet
ρ	fluid weight density, pound / feet^3
ΔP	pressure change, psi

INTRODUCTION

The method of characteristics (MOC) is a generally accepted technique to analyze fluid transients in pipes (Streeter [1], Schohl [2]), but this technique tacitly assumes that the pipe is full of water or that a known volume of air is trapped in the pipe. How does air bubbling up into a long pipe with one end open to atmospheric pressure affect fluid transients? Referring to Fig. 1, fluid transients, or pressure surges, occur when the pump is started or stopped or the valves are opened or closed to change the flow rate. To perform a fluid transient analysis, the boundary conditions need to be determined. That is, how much air is in the system at any specified time and where is the air located. This paper will consider that question and show that the time required for the air to travel along the pipe length is significant with respect to transient phenomena. Although trapped air in a pipe is known to reduce the maximum pressure surge, the surge typically occurs long before air flow into the pipe can affect the surge.

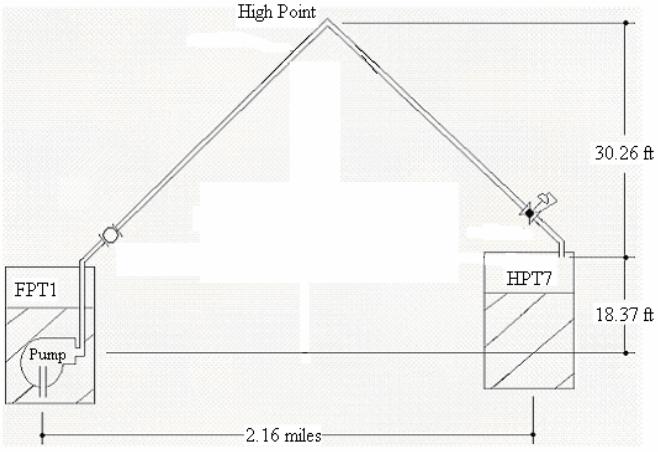


Figure 1: System Schematic

In short, this paper presents various experimental results and calculations for a system installed at Savannah River Site in South Carolina. First, experimental results describe air entrainment into a vertical tube when the upper end of the filled tube is suddenly opened. Second, experimental results and calculations are compared to describe

fluid flow and air entrainment into a 2.16 mile long pipe, which has an intermediate high point. Finally, various fluid transient calculations are performed to understand what happens in the system when valves and pumps are actuated.

EXPERIMENTAL RESULTS FOR AIR ENTRAPMENT IN A VERTICAL TUBE

What happens when the upper end is opened on a liquid filled vertical tube with an intermediate high point, as shown in Fig. 2. That is, when the liquid comes to rest is vapor or air present at the high point in the tube? Using a flexible ¾ inch diameter tube, the answer is experimentally shown here that air displaces the water, unlike observations for a small diameter tube.

For a small diameter tube initially filled with the upper end closed, the system acts as a one dimensional model, as shown in Fig. 3. Considering the mass balance, the pressure near the top of the tube equals the vapor pressure, and the pressure at the bottom of the tube equals atmospheric pressure. At standard conditions, the vapor pressure equals approximately 0.3 psi and the atmospheric pressure is 14.7 psi. The pressure due to the height of the fluid plus the vapor pressure equals atmospheric pressure, such that the expected maximum height of fluid in the column approximately equals 33.3 feet. When a small diameter tube is lifted such that the bottom of the tube is exposed to atmosphere, the tube remains full to establish the initial conditions for test. This condition is sometimes referred to as the straw effect. You put your finger over the end of a straw and remove to from a glass and it remains full. If the tube is of large diameter, the liquid flows out of the tube and is displaced by air.

To investigate air entrapment in a tube, the dimensioned test setup shown in Fig. 2 was used. A ½ inch diameter, flexible plastic, Tygon tube was mounted vertically, filled completely with water, and each end of the tube was closed prior to tests. Three tests were performed and the results are shown in Figs. 4 – 6. The bold line shows the final location of water in the tube, and the sequence of opening the two tube ends for each test is also shown in the figures. Since the tubing collapsed under vacuum, the presence of air or water vapor in the tube was visually verified. The tube sections in the figures containing air at equilibrium are shown unbolded. When the valves were initially opened the water flowed back and forth in the tubing, first creating a vacuum in the tube as the water exited the tube, and then creating air pockets in the tube as air flowed back through the water in the tube to fill the void. The process was complete in less than a minute for each case. For the test shown in Fig. 6, most of the water drained immediately and was displaced by air on opening the lower end of the tube. Note that in each case, air was entrapped in the tubing, which is not predicted by using a one dimensional mass balance. The one dimensional assumption is only valid when both ends of the tube are submerged in water or for small diameter tubes with one exposed end.

Considering these results and referring again to Fig. 1, bubbling of air up through the pipe from the right is expected after a pump shutdown, and the pipe is expected to drain completely over time. Additionally, the pipe may tend toward open channel flow under some conditions. Test results from the actual pipe system provide further insight into air entrapment, but the added complexities of fluid transients need to be factored in, and a system description is required.

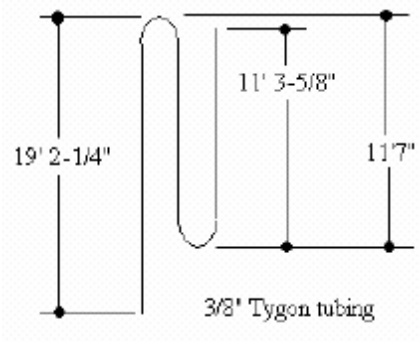


Figure 2: Test Setup

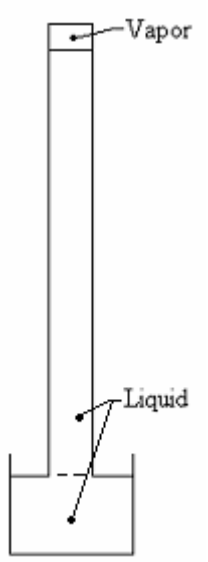


Figure 3: One Dimensional Model of Vapor Formation in a Vertical Tube

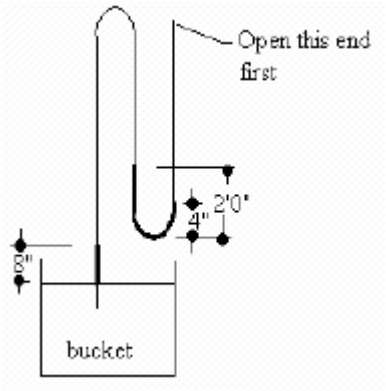


Figure 4: Submerged Tubing End

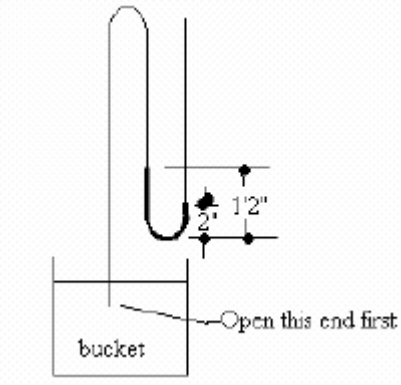


Figure 5: Submerged Tubing End

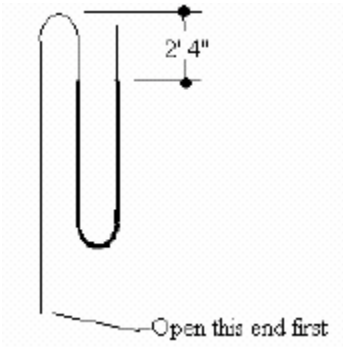


Figure 6: Non-submerged Tubing End

SYSTEM DESCRIPTION

The system process diagram is shown in Figs. 1 and 7, where a 2.16 mile long, 3 inch NPS, stainless steel pipe connects two, twelve foot diameter tanks referred to as FPT1 and HPT7 (≈70.5 gallons per inch). The system is used to transfer water or nuclear waste with a specific gravity of approximately 1.2 between the two tanks using a pump mounted on top of FPT1. The pump curve is shown in Fig. 8; the motor torque vs. speed curve in Fig. 10; and the pump installation in Fig. 9. The operating motor conditions dictate the steady state flow rate, and the constant pump speed is controlled using a variable frequency drive at 1800 rpm, which is an actual speed of 1784.9 rpm when compensated for motor slip.

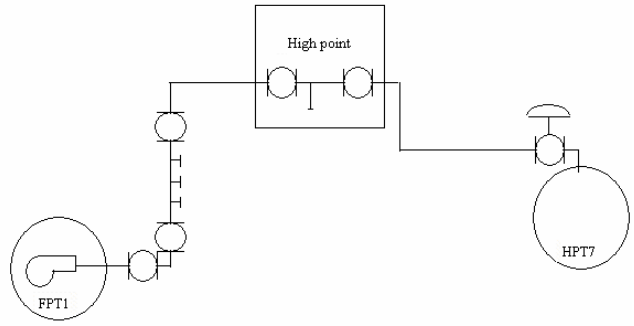


Figure 7: System Process Diagram

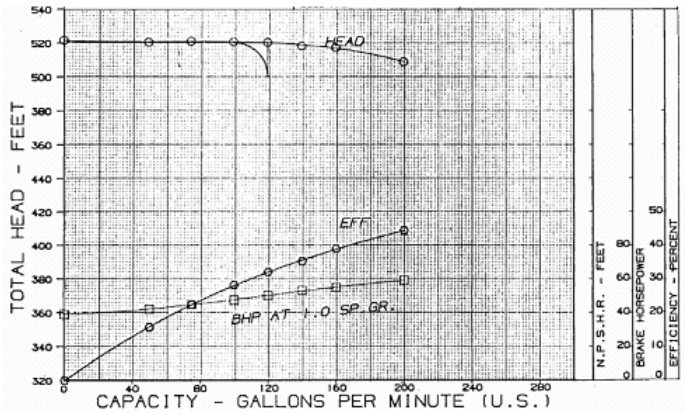


Figure 8: Pump Curve at 2385 rpm (Operating Speed = 1800 rpm)

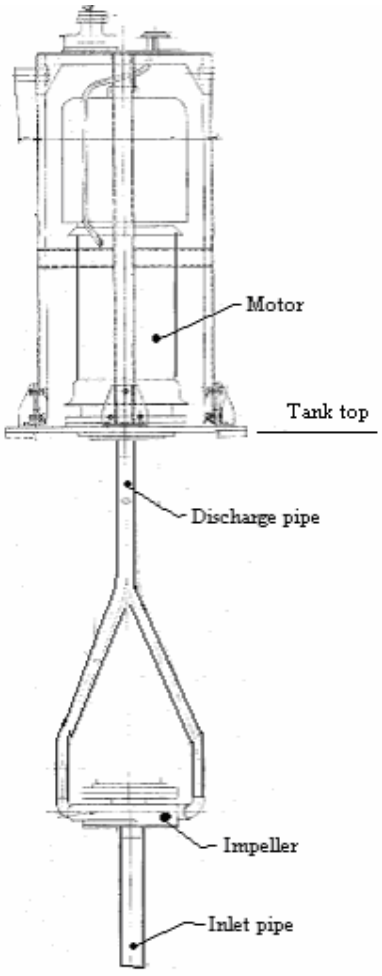


Figure 9: Pump installation (Lawrence Pumps, Inc.)

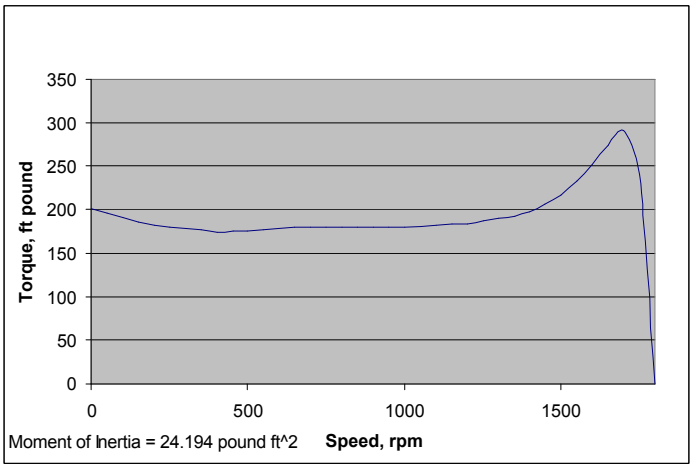


Figure 10: Motor Torque / Speed Curve

FLOW RATES AND MAXIMUM PRESSURES

Flow rates change throughout the transfer process, but steady state flow rates provide a basis for comparison between theory and experiment. The measured, maximum, steady state flow rate is 70 gallons per minute for waste and 100.1 gpm for water, and flow takes 32 minutes to reach HPT7 after starting the pump at FPT1, as shown in Fig. 11. The 104.9 gpm calculate steady state flow rate for water is less than 5% above the measured flow rate. Initial flow rates are needed to estimate pressure spikes in the system.

Measured Flow Rates

Measured flow rates were determined during a water transfer, as recorded in Fig. 11. Measured flow rates of 70 gpm for a waste transfer were also recorded in the facility but the records are not included here. When the pump was started for the water transfer (pump startup), the level decreased in FPT1 and the pipeline to HPT7 was filled until water reached HPT7 (Flow into HPT7). Steady state flow occurred for five minutes until the pump was stopped. Prior to pump shutdown, steady state flow into HPT7 was measured at 98.7 or 100.1 gpm. When the pump was shut down, flow separated at the high point and flowed in both directions, as indicated by level increases in both tanks. Immediately after pump shutdown the flow rate into HPT7 was 12.6 gpm and the flow rate into FPT1 was 19.1 gpm. The flow rate never exceeded 22 gpm in either direction after pump shutdown. The flow rates progressively decreased and then sharply increased about an hour and twenty five minutes after pump shutdown. The pump tanks continued to fill for more than two hours, and draining of the pipeline only stopped when valves in the pipeline were closed to stop the transfer. Draining would have continued until the pipe was emptied.

Data was recorded at various intervals of one to seven minutes, using the Process Information system (PI [3]). Measurement uncertainty is attributed to the measuring devices, which consisted of dip tubes, or bubblers, which typically have accuracies of ± 2% for each bubbler. These devices bubble air into solution using vertical tubes submerged in the tank. Using several bubblers, the pressures required to bubble air into solution are measured to determine the fluid levels and specific gravity of the fluid. Note that two levels are recorded for HPT7, and that the difference in levels is significant. The disparity between them increases from 3 to 9 inches throughout the 90 inch range of interest. Even though errors exist in the level measurements, the difference in measured flow rates is less than 1.5%. Consequently, measured flows can be validly compared to calculated flow rates.

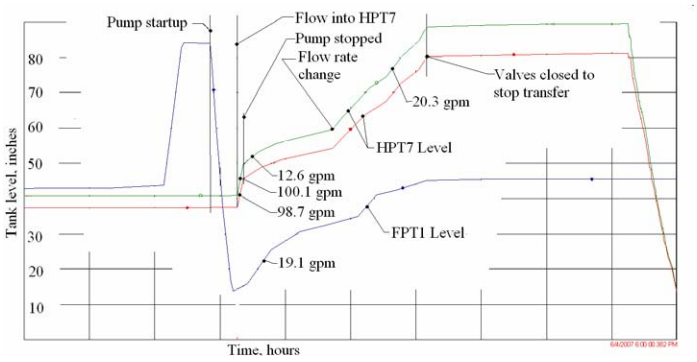


Figure 11: Tank Level Changes During A Water Transfer

Maximum Pressure Surges Based on Measured Flow Rates

The maximum pressure spikes in the system due to a suddenly closing valve were calculated, and are tabulated in Table 1 with pertinent material properties. Three cases are listed for the condition where the downstream valve at HPT7 is suddenly closed. The first considers closing the valve while the pump is operating and water is being transferred. The second considers closing the valve while the pump is transferring waste; and the third considers closing the valve after the pump is shutdown during a water transfer. Pressure surges are significantly higher when the valve is closed during pump operation, and pressure surges are slightly higher for a water transfer than a waste transfer.

Modulus of Elasticity, E, psi, 304L, ASME B31.3	28,300,000
Bulk Modulus, water, k, psi (Avalone and Baumeister [4])	319,000
Bulk Modulus, salt water, k, psi (Salt water properties assumed for waste. Experimental values unavailable)	344,000
Density, water, pound / foot^3, ρ	62.4
Density, waste, ρ, pound / foot^3, (SpG = 1.2)	87.36
Poisson's Ratio, ν	0.3
Inside pipe diameter, inches, ID	3.068
Outside pipe diameter, inches, OD	3.5
Velocity, V, feet /sec, water, (100.1 gpm)	4.34
Velocity, V, feet /sec, water, (22 gpm)	0.95
Velocity, V, feet /sec, waste (70 gpm)	3.038
Wave speed, a, feet /sec, water	4487
Wave speed, a, feet /sec, waste	4229
Pressure increase, ΔP, psi, Suddenly closed valve, water, (100.1 gpm)	262.5
Pressure increase, ΔP, psi, Suddenly closed valve, water, (22 gpm)	57.7
Pressure increase, ΔP, psi,, Suddenly closed valve, waste (70 gpm)	207.6

Table 1: Pressure Surges Based on Measured Flow Rates

The relationships between the sudden pressure increase, the flow rate, and the density for a suddenly closed valve are described by Eqs. 1 and 2 (Streeter and Wiley [1]), such that

$$\Delta P = \frac{\rho \cdot a \cdot V}{g} \qquad (1)$$

The equation for the acoustic wave speed, a, in the fluid filled pipe assumes that the thick wall pipe is fixed throughout its length.

$$a = \sqrt{\frac{\frac{k \cdot g}{\rho}}{1 + \frac{k \cdot D}{E \cdot t} \cdot \left[\frac{2 \cdot t}{D} \cdot (1 + \nu) + \frac{D \cdot \left(1 - \nu^2\right)}{D + t} \right]}} \qquad (2)$$

where D is the average diameter, ΔP is the pressure rise, ρ is the density, E is the modulus of elasticity of the pipe, k is the bulk modulus of the fluid, ν is Poisson's ratio for the pipe material, V is the initial velocity of the fluid in the pipe, and g is the gravitational constant.

Comparing water and waste transfers, the velocity is larger for water than waste (100.1 gpm > 70 gpm), and the specific gravity, or density, is lower for water than waste (1 < 1.4). Fluid transient calculations for the lower velocity waste transfers are not considered in detail here, as water transfers provide significantly higher velocities and consequent higher pressure surges since pressure magnitudes are proportional to flow rates. By substitution of terms into Eq. 1, the pressure increase due to a suddenly closed valve in a waste filled pipe is 79% of the pressure increase in a water filled pipe, and the effects of velocity differences on ΔP therefore offset the effects of material differences. In other words, calculated flow rates during water transfers provide upper, bounding estimates for pressure magnitudes in the pipe system.

Calculated Flow Rates

The calculated, steady state flow rate for a water transfer was found to be104.9 gpm from the TFSIM fluid transient solver (Schohl [2]). The solver assumes incompressible, one-dimensional flow, using Darcy-Weisbach friction factors. Since the pump and motor characteristics are already defined, all that is required are the friction coefficients, K, for the minor loss components, which are listed in Table 2. The grade varies between 0.27 % and 1.39 % in the pipe connecting the high point and the two pump tanks, and elevations are shown on Fig. 1. Flow rates following pump shutdown were measured but could not be accurately calculated due to air entrainment considerations.

Pipe Section	Length, feet Roughness = 0.00015 Avalone [4]	Elbows, 50" radius K = 0.756 Crane [5]	Ball valves, McCanna, Cv =420 K = 0.054 Crane [5]	Tees K = 1.08 Crane [5]
FPT1	20	15	3	3
Piping between FPT1 and high point	6350	3	3	1
High Point	10	5	2	---
Piping between HPT7 and high point	6605	5	2	---
HPT7	20	5	1	---

Table 2: Friction Data

AIR ENTRAINMENT

The information above provides some understanding of air entrainment in the pipe system. The transfer was in process at 100 gpm when the pump stopped. Flow immediately separated by vaporization at the high point, and water flowed in both directions. The sub-atmospheric pressure (-14.4 psig) in the vapor cavity caused the velocity of the fluid to progressively slow down for more than an hour, as some of the water drained into HPT7. The flow rate then increased, due to air bubbling up into the pipe. To support this statement the tube experiment requires comparison to the transfer pipe.

Air was noted to fill the tube in less than a minute, which implies that the air velocity was between 1/4 and 1/2 foot per second. The average velocity required for the air to reach the vapor space was 0.6 ft per second (3306 ft / 88 minutes = 0.6 ft / sec). The air flow rates are nearly the same for either system. Essentially, the flow in the pipe approaches open channel flow momentarily as the air enters the upstream void in the pipe. When the air enters the void, the pressure increases toward atmospheric, the restraining vapor pressure is reduced, and the pipe flows full again. In a long pipe, this process may repeat itself while the pipe drains. The concise effects of the air pressure changes on the vapor space and flow rate cannot be calculated, but this description of air entrainment is consistent with the basic theory of open channel flow.

Open channel in the pipe flow may occur when the downstream head exceeds the upstream head (Avalone and Baumeister [4]). That is, open channel flow in a steady state system occurs when

$$\frac{P_u}{\rho} + Z_u < \frac{P_d}{\rho} + Z_d \qquad (3)$$

where P_u and P_d are the upstream and downstream pressures respectively, and Z_u and Z_d are the upstream and downstream elevations respectively.

The fact is that the upstream vacuum which occurs at pump shutdown provides a sufficient condition for open channel flow to occur at any time during draining of the pipe. All that is required is that the air at the downstream end of the pipe has time to move throughout the pipe length to establish open channel flow. Once open channel flow is established, the vacuum is reduced, and the pipe flows full again until open channel flow is reestablished.

In short, the system dynamics following pump shutdown are extremely complex. First, a vapor pocket forms and flow moves in both directions from the high point. Then, air moves into the vapor space when the pipe flows partially full, followed by full pipe flow. Models to describe this behavior are unavailable, but an understanding of the system behavior permits limited use of the available MOC technique to describe fluid transients.

FLUID TRANSIENT CALCULATIONS

Several examples of fluid transients during water transfers are considered for closing the valve at HPT7 at different speeds and conditions. Pump shutdown cannot be modeled for this system. The MOC assumes that both ends of the pipe are submerged, and does not account for water which permanently exits the pipe.

Valve Closure at HPT7

The MOC solution for fluid transients (TFSIM) provides valid results for valve closures while the pump is operating, since air is not introduced into the system. Pressures at various points along the pipe are shown in Figs. 12 – 14. The highest pressures occur at the valve as it closes. Altering the valve closure time significantly affects the pressure surge. A one second closing time is used for sudden closure of the downstream valve near HPT7. Figure 15 shows the valve characteristics as a function of flow versus valve opening, and the effects of different linear closing times from 20 seconds to 4 minutes are shown in Figs. 16 – 18. Although all of the air is expected to be expelled from the piping while it fills, the effects of a small amount of entrapped air are shown for illustration only in Fig. 19. By comparing Fig. 14 to Fig. 19, those effects are seen to be negligible at the valve, since the air is not located at the valve.

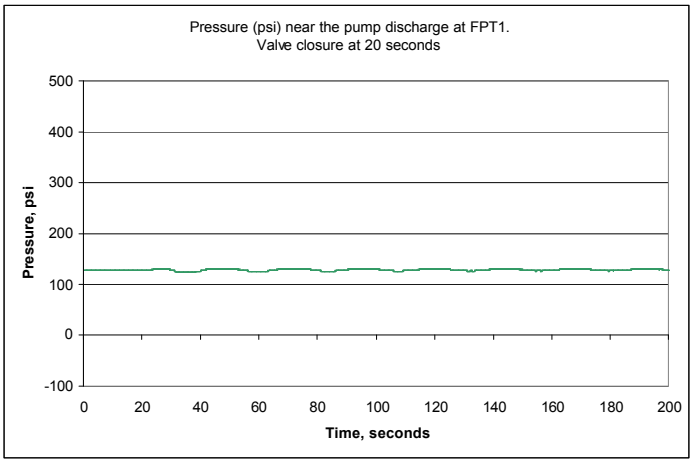


Figure 12: Pressures Near the Pump for a Sudden Valve Closure, Pump Operating

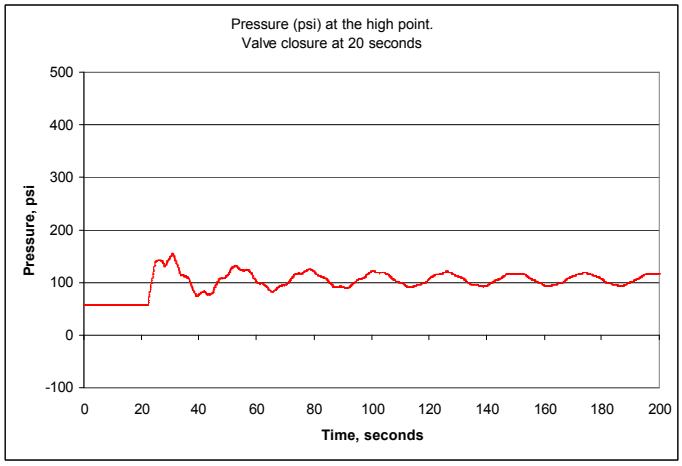


Figure 13: Pressures at the High Point Near the Middle of the Pipeline for a Sudden Valve Closure, Pump Operating

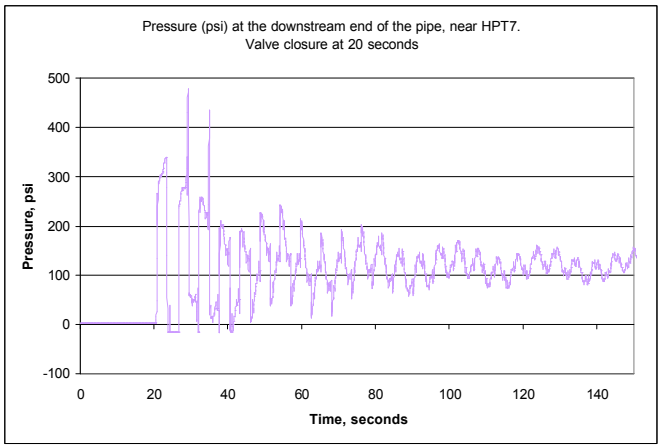


Figure 14: Pressures Near the End of the Pipeline Upstream of the Closing Valve for a Sudden Valve Closure, Pump Operating

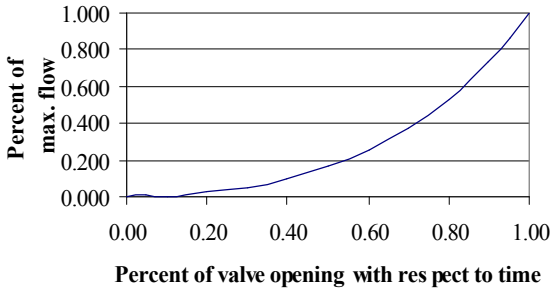


Figure 15: Full Port, Ball Valve Characteristics

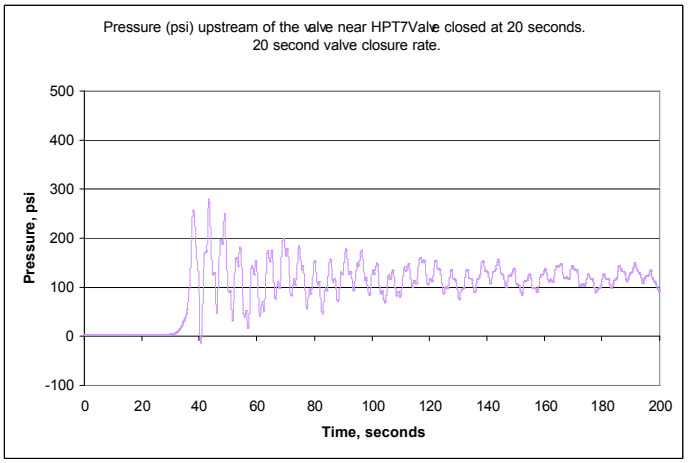


Figure 16: Pressures Near the Valve at HPT7 for a 20 Second Valve Closure, Pump Operating

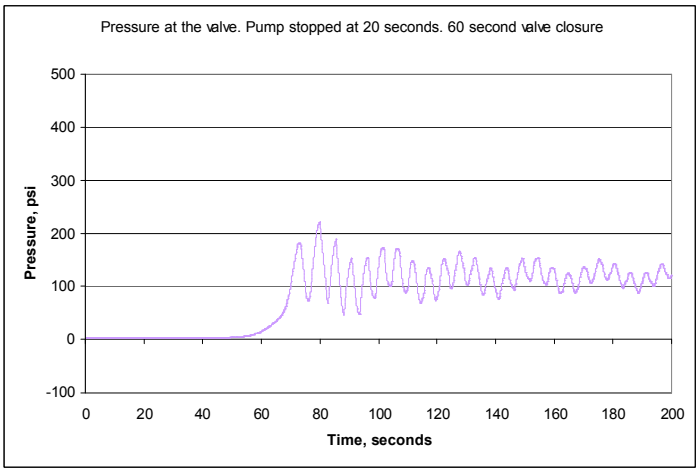


Figure 17: Pressures Near the Valve at HPT7 for a 60 Second Valve Closure, Pump Operating

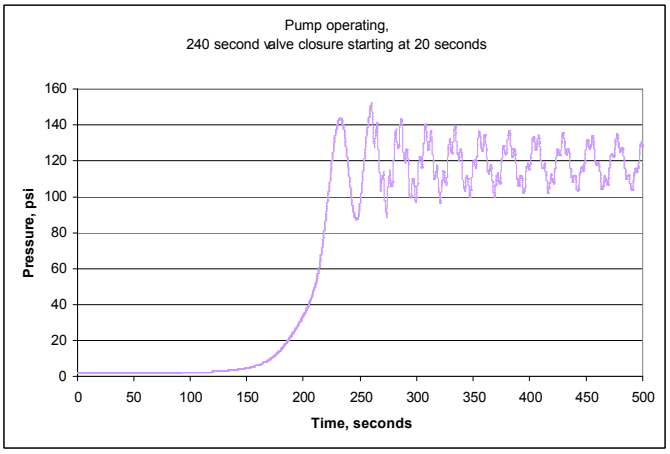


Figure 18: Pressures Near the Valve at HPT7 for a 240 Second Valve Closure, Pump Operating

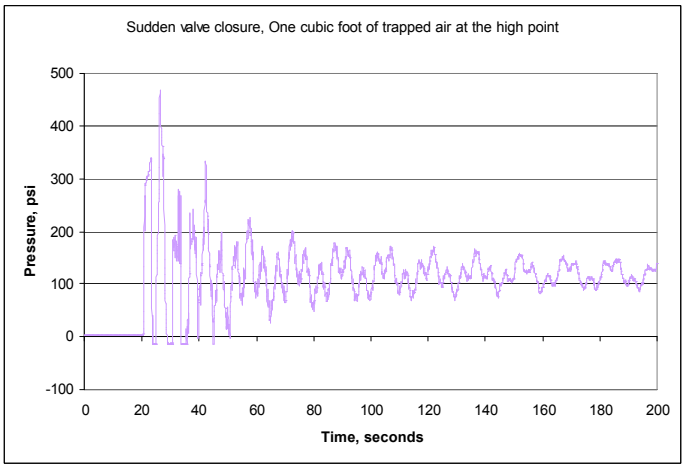


Figure 19: Pressures Near the Valve at HPT7 with One Cubic Foot of Air at the High Point, Sudden Valve Closure, Pump Operating

Models for Pump Shutdown, Valve Closure, and Pump Restart

Without a working model, predicting the system performance shown in Fig. 11 is, at best, problematic. Even so, the MOC approach and the basic water hammer equations can be used to provide some limited insight into what happens when valves are closed following a shutdown or the pump is restarted. Specifically, the MOC technique can be used to provide limiting cases describing the transients for a similar system, which is the same except that both ends of the pipe are submerged. In comparison to this technique, the maximum obtainable flows were considered for the case where air is assumed to be present at the high point and vapor is absent, which is simply a gravity drain of the system. The actual flow conditions exist between these two disparate conditions.

Numerous models were required to investigate valve and pump operations, and a comparison of the various models follows discussions of each model. That is, the maximum pressures due to different operating conditions are examined using the MOC and gravity drain models, which are compared to calculations of the maximum pressure surge calculated from the experimental data from pipeline testing.

Pump Shutdown, MOC Calculation for a Pipe with Both Ends Submerged. Figures 20 and 21 are obtained by modeling the 2.16 mile pipe using the MOC, and assuming that both pipe ends are submerged. Note that the transient event occurs in less than a minute and a half as the pressures in the pipe decrease to zero. The flow rates rapidly decrease from 104.9 gpm through zero, and a reverse flow then occurs. Near HPT7, the reverse flow converges to a nearly steady flow of -11.7 gpm. . The vapor space does not collapse, since the flow rate at the pump remains higher than the flow rate at the other end of the pipe. A siphon is established from the higher tank to the lower tank, while the shrinking vapor space remains in the pipe. Also, when the system is modeled for the case of a non-operating pump, a siphon would flow at 24.55 gpm from HPT7 to FPT1. Accordingly, the equilibrium siphon rate is lower when the MOC technique is used. In the actual system, a siphon cannot exist since there is an air break at the higher tank (HPT7).

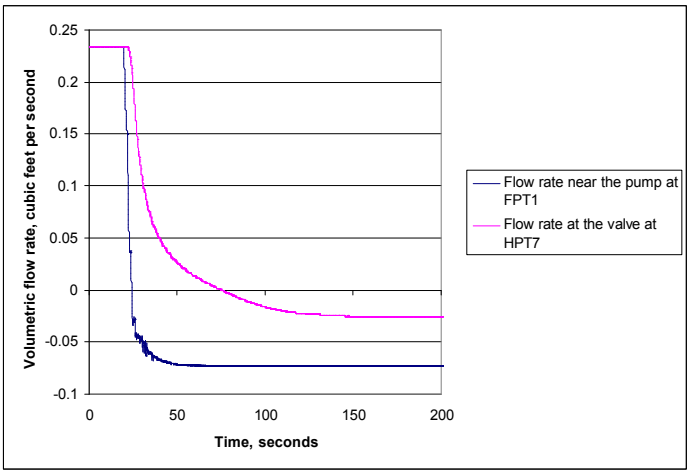


Figure 20: Volumetric Flow Rates at Pump Shutdown at 20 Seconds for a System with Both Pipe Ends Submerged

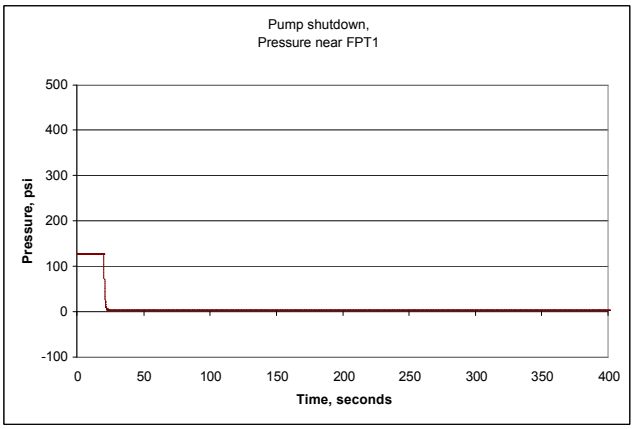


Figure 21: Pressures at Pump Shutdown at 20 Seconds for a System with Both Pipe Ends Submerged

Comparing Figs. 11 and 20, the MOC solution is obviously incorrect. The flow rates in the real system do not converge to zero and then siphon to the FPT1 low point in the system. The flow rates in the real system reverse direction only one time at the high point, and the flows then continue into both tanks. The suction on the opposing flow streams due to vaporization at the high point is inadequate to overcome gravitational and air entrainment effects.

Valve Closure After Pump Shutdown, MOC Calculation for a Pipe with Both Ends Submerged. Pressure transients due to different valve closure times after a pump shutdown are shown in Figs. 22 and 23. Pressure transients near HPT7 due to different valve closure times are shown in Figs. 21 and 22. Overall, pressure transients are significantly diminished as the flow rate decreases.

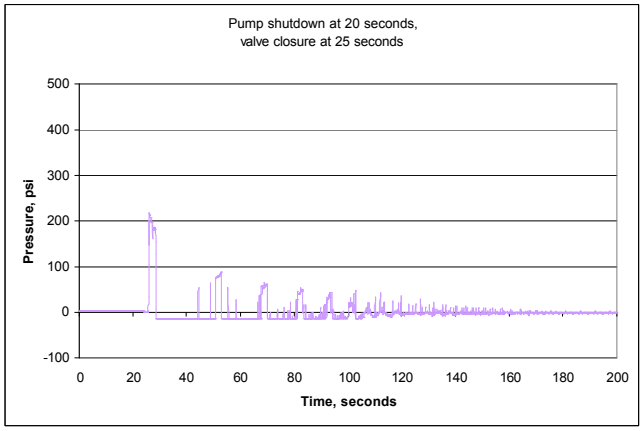


Figure 22: HPT7 Valve Closure Immediately After Pump Shutdown

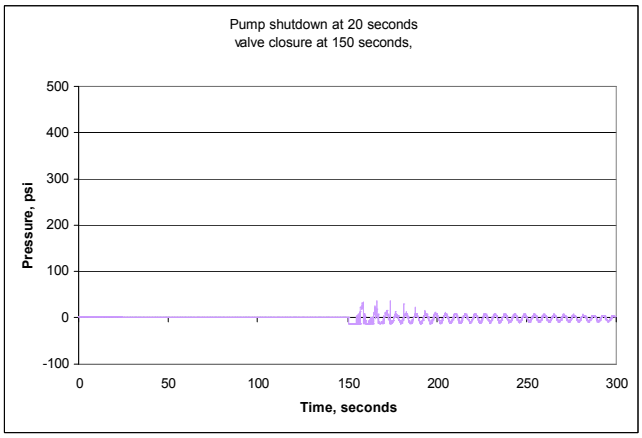


Figure 23: Sudden Valve Closure After a Low Velocity Siphon Commences

Pump Restart, MOC Calculation for a Pipe with Both Ends Submerged. For pump restart, the MOC approach is provided for illustration to better understand the complex fluid transients of this system. In Fig. 24 the flow is still moving when the pump is restarted and the pressure surge is minimal. If the flow was temporarily arrested due to a valve closure, the pressure surge is significantly higher when the pump is restarted, as shown in Fig. 25.

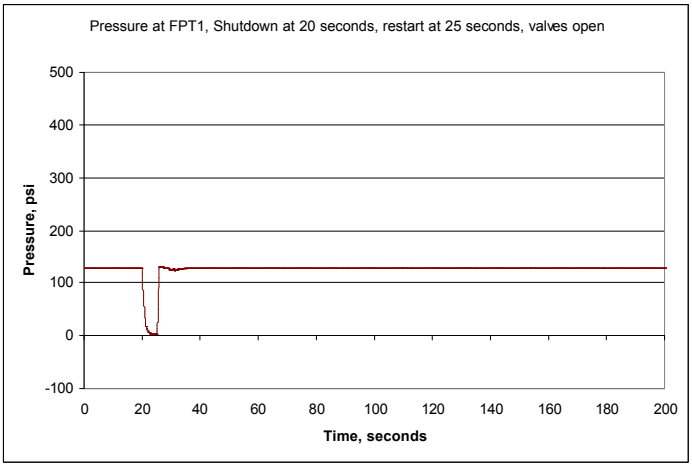


Figure 24: Pressures for a Pump Restart

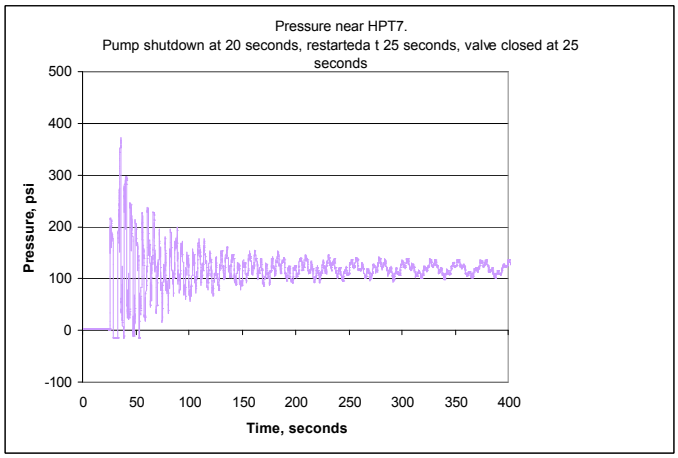


Figure 25: Pressures for a Pump Restart and Simultaneous, Sudden Valve Closure

Pump Shutdown for the Case of Air Entrainment at the High Point (Gravity Drain Model). If one assumes that flow reverses direction at the high point when the pump is shut down, and that gravity is the only force moving the fluid in the pipe, an upper limit to the flow rate can be determined for this example. While this assumption is untrue for the minute or two immediately following pump shutdown, this assumption limits the nearly steady state flow condition established in the real system. The pipe system is modeled as two separate pipe systems, as shown in Fig. 26, using the same components used for the complete system model. Under these conditions, the flow rates are 42.04 gpm from the high point to HPT7 and 58.13 gpm from the high point to FPT1, which are both considerably higher than the observed maximum flow rate of 22 gpm. Once again, the MOC does not consider air entering the pipe.

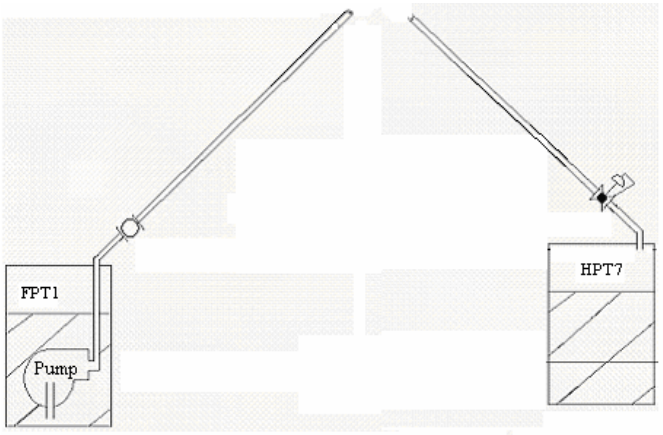


Figure 26: Gravity Drain Models

Valve Closure After Pump Shutdown for the Case of Air Entrainment at the High Point. Pressure transients can be calculated using the MOC and the model shown in Fig. 26. Note that pressure surges due to a valve closure for the drain to FPT1 was calculated using a valve closure at FPT1 instead of the typical valve closure at HPT7 used throughout this paper. The results are shown for sudden valve closures in Figs. 27 and 28.

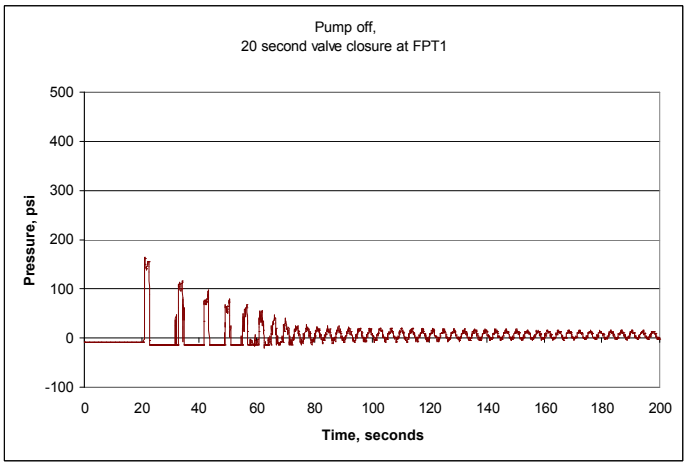


Figure 27: Sudden Valve Closure at FPT1, Gravity Drain Model

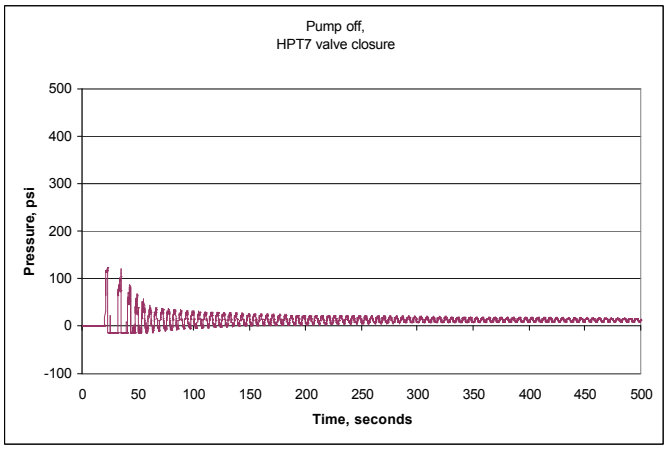


Figure 28: Valve Closure at HPT7, Gravity Drain Model

Transient Pressure Determinations From Experimental Data

Steady state flow can be used to estimate the maximum pressure surge on restarting the pump. Using the FPT1 model in Fig. 26, flow is assumed only between FPT1 and the high point. Using the same model parameters the flow rate is determined to be 157.1 gpm before flow starts downhill toward HPT7. Since liquid is in the downstream pipe section, the two liquid sections will collide somewhere along the pipe length. Conservatively assuming that the collision takes place near the high point, the 157.1 gpm flow rate can be substituted into the water hammer equation for a liquid-liquid impact, which is one half of Eq. 1, such that

$$\Delta P = \frac{\rho \cdot a \cdot V}{2 \cdot g} = 206_psi \qquad (4)$$

The flow is assumed to move after valves are opened similar to the 12.6 gpm flows observed in Fig. 11. Then

$$\Delta P = \frac{\rho \cdot a \cdot V}{2 \cdot g} = 189.5_psi \qquad (5)$$

COMPARISON OF PRESSURE CALCULATIONS BASED ON EXPERIMENT AND THEORY

Numerous models were considered, and the maximum pressure surges determined for those models are summarized in Table 3. The value of the maximum surge is determined as shown in Fig.29, and the pressures indicated in bold face print are considered to be valid estimates for pressure transients. The other pressures in the table are errant. Those based on the MOC improperly describe the flow, and those based on gravity draining over estimate pressure surges by as much as 283 percent. Results for the maximum pressure surges can be summarized by stating that a 262.5 psi pressure will occur when a valve is closed while a pump is operating; a 57.7 psi surge will occur when a valve is closed several minutes after a pump is stopped; and a 189.5 psi surge may occur if the pump is restarted after a shutdown.

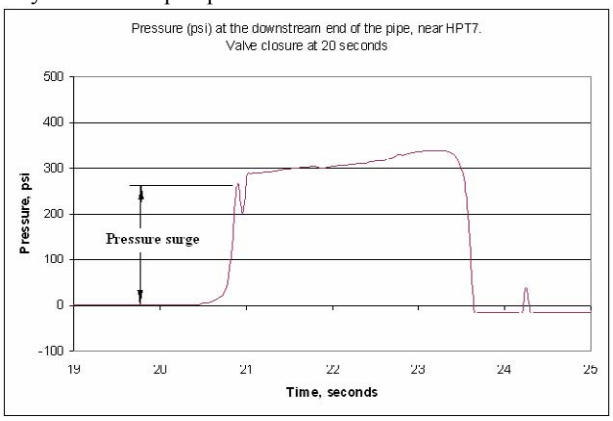


Figure 29: Determination of Pressure Surge Magnitudes

CONCLUSIONS

Air entrainment significantly affects fluid transients. Experimental data was obtained describing the complex relationship between vapor formation, air entrainment, and flow rates during valve and pump operations in piping with one end open to atmospheric pressure. The experiments consisted of a 41 foot long by ¾ inch diameter, vertical tube and a 2.16 mile long by 3 inch diameter pipe with an intermediate high point.

Analytical results were compared to experimental data, using MOC models and gravity drain models. In some cases the MOC can be used to describe the pressure transients following valve closure, but for these systems with one end of the pipe open to atmosphere, the classical MOC technique is inadequate to properly describe the flow changes and resulting pressure transients in the pipe when a pump is shut down. If experimental measurements of the flow are available, the pressure surges on restart of the pump or valve closures following pump shutdown can be accurately discerned using basic water hammer equations, but in the absence of experimental data only rather high estimates of the pressure surges during shutdown and restart can be determined. In fact, pressure estimates were significantly over-conservative by a factor of as much as 2.8 unless experimental field data was available to evaluate pump operations. At present, theory alone is inadequate to fully describe the dynamics of fluid flow when a pump shuts down in a pipe system with one end open to atmospheric pressure.

REFERENCES

1. Wiley, E. B., and Streeter, V. L., 1982, "Fluid Transients", FEB Press, Michigan, pp. 1 – 161.
2. Schohl, G., 1998, Users Manual for Locksim, Hydraulic Simulation of Navigation Lock Filling and Emptying Systems", Tennessee Valley Authority, pp.1 – 191.
3. Plant Information Systems, 2000, OSI Software Inc., San Leandro, Cal.
4. Avalone, E. Baumeister, "Mark's Standard Handbook for Mechanical Engineers", 1978, McGraw Hill, N. Y. p. 3-68.
5. Crane, 1988, Technical Paper Number 410, "Flow of Fluids Through Valves, Fittings, and Pipe", Chicago, pp. A-26 to A-29.

Transient conditions					Fig. / Eq. / Table	Pressure psi
Model	Pump	Shut down	Sudden valve closure	Restart		
MOC	on	no	yes	C	Fig. 14	**289**
MOC, air trapped at the high point	on	no	yes	n/a	Fig. 19	**289**
Experimental	on	no	yes	n/a	Tab. 1	**262.5**
Gravity drain / 24.55 gpm Siphon	on	no	yes	n/a	24.55 gpm	64.4
MOC	on	no	no, 20 second closure	n/a	Fig. 16	**246.9**
MOC	on	no	no, 60 second closure	n/a	Fig. 17	**177.4**
MOC	on	no	no, 240 second closure	n/a	Fig. 18	**142.5**
MOC, FPT1 gravity drain	off	n/a	yes	n/a	Fig. 27	163.5
Experimental FPT1 drain	off	n/a	yes	n/a	Tab. 1, 22 gpm	**57.7**
MOC, HPT7 gravity drain	off	n/a	yes	n/a	Fig. 28	121
Experimental HPT7 drain	off	n/a	yes	n/a	Tab. 1, 22 gpm	**57.7**
MOC, Gravity drain	on	yes	open	no	Fig. 21, 11 gpm-32 gpm	**128.40**
Experimental	on	yes	open	no	Fig. 11, 22 gpm	----
MOC	on	yes	open	yes	Fig. 24	130.8
Experimental	on	yes	open	yes	Eq. 4	206
Gravity drain	on	yes	open	yes	Eq. 5	**189.5**
MOC	on	yes	yes	yes	Fig. 25	257
Gravity drain	on	yes	yes	yes	Eq. 5	**189.5**

Table 3: Summary of Transient Models and Maximum Pressures